

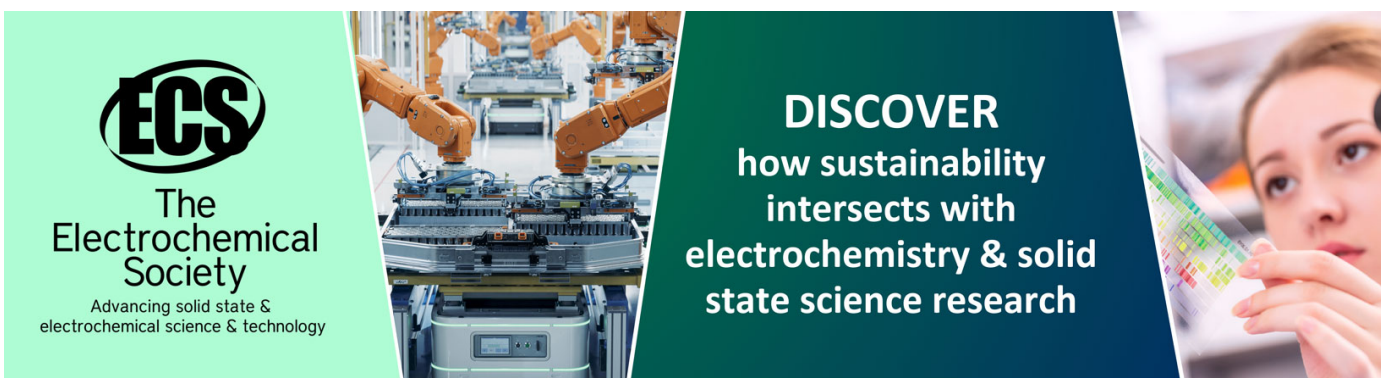
Nanoengineering a single-molecule mechanical switch using DNA self-assembly

To cite this article: Ken Halvorsen *et al* 2011 *Nanotechnology* **22** 494005

View the [article online](#) for updates and enhancements.

You may also like

- [\(Invite\) Insights in Measuring Particle Size of Multiatomic Nanoparticles By XAS](#)
Nebojsa Marinkovic, Kotaro Sasaki and Radoslav R. Adzic
- [Special issue on applied neurodynamics: from neural dynamics to neural engineering](#)
Hillel J Chiel and Peter J Thomas
- [Advancing agricultural greenhouse gas quantification](#)
Lydia Olander, Eva Wollenberg, Francesco Tubiello et al.



ECS
The
Electrochemical
Society
Advancing solid state &
electrochemical science & technology

DISCOVER
how sustainability
intersects with
electrochemistry & solid
state science research

Nanoengineering a single-molecule mechanical switch using DNA self-assembly

Ken Halvorsen^{1,2,3}, Diane Schaak¹ and Wesley P Wong^{1,2,3}

¹ The Rowland Institute at Harvard, Harvard University, Cambridge, MA, USA

² The Immune Disease Institute/Program in Cellular and Molecular Medicine, Children's Hospital Boston, Boston, MA, USA

³ The Department of Biological Chemistry and Molecular Pharmacology, Harvard Medical School, Boston, MA, USA

E-mail: wong@rowland.harvard.edu

Received 9 June 2011, in final form 25 July 2011

Published 21 November 2011

Online at stacks.iop.org/Nano/22/494005

Abstract

The ability to manipulate and observe single biological molecules has led to both fundamental scientific discoveries and new methods in nanoscale engineering. A common challenge in many single-molecule experiments is reliably linking molecules to surfaces, and identifying their interactions. We have met this challenge by nanoengineering a novel DNA-based linker that behaves as a force-activated switch, providing a molecular signature that can eliminate errant data arising from non-specific and multiple interactions. By integrating a receptor and ligand into a single piece of DNA using DNA self-assembly, a single tether can be positively identified by force–extension behavior, and receptor–ligand unbinding easily identified by a sudden increase in tether length. Additionally, under proper conditions the exact same pair of molecules can be repeatedly bound and unbound. Our approach is simple, versatile and modular, and can be easily implemented using standard commercial reagents and laboratory equipment. In addition to improving the reliability and accuracy of force measurements, this single-molecule mechanical switch paves the way for high-throughput serial measurements, single-molecule on-rate studies, and investigations of population heterogeneity.

 Online supplementary data available from stacks.iop.org/Nano/22/494005/mmedia


(Some figures in this article are in colour only in the electronic version)

1. Introduction

The ability to precisely manipulate individual molecules has led to stunning new discoveries in physics, biology, and medicine [1, 2], as well as powerful new methods in nanoscale engineering. For example, single-molecule force measurements have revealed the basic mechanical properties of nucleic acids [3], the dynamics and functioning of molecular motors [4, 5], and the role of hydrodynamic forces in the circulatory system in regulating enzymatic

activity [6]. In addition, these measurements have yielded fundamental insights into the dynamical strength of molecular interactions [7], which have led to the development of creative new tools for nanoscale assembly [8].

Mechanical forces can be applied to individual molecules using a broad range of tools, including optical traps, magnetic tweezers, mechanical cantilevers, and the centrifuge force microscope [9, 10] (figure 1). Yet a common requirement of these methods is that single-molecule constructs must be specifically tethered between two surfaces (e.g. beads, cover slips or cantilevers) to enable their manipulation and detection. This leads to one of the major challenges in single-molecule experimentation—verifying that exactly one molecular tether is being pulled, and distinguishing this tether from non-specific

 Content from this work may be used under the terms of the [Creative Commons Attribution-NonCommercial-ShareAlike 3.0 licence](http://creativecommons.org/licenses/by-nc-sa/3.0/). Any further distribution of this work must maintain attribution to the author(s) and the title of the work, journal citation and DOI.

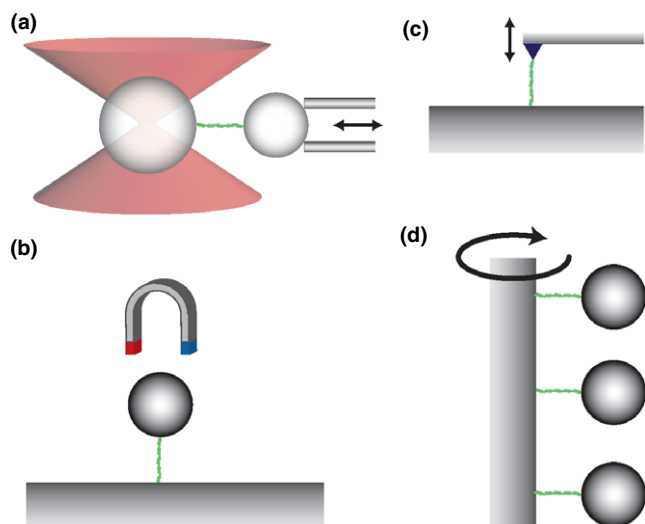


Figure 1. Single-molecule manipulation techniques include those of (a) optical tweezers, (b) magnetic tweezers, (c) the atomic force microscope, and (d) the centrifuge force microscope.

and unintended interactions that may occur (e.g. surface–surface interactions, formation of multiple bonds). The success and reliability of single-molecule experiments depends upon the creation of reliable, verifiable and robust linking techniques. This is particularly important for bond rupture studies (e.g. characterizing the strength of molecular adhesion bonds [11], DNA base pairing [12], and cell adhesion and signaling [13]), as the dissociation between two molecules can be difficult to positively identify due to the lack of an obvious mechanical signature.

We have met this experimental challenge with a new single-molecule attachment technique that facilitates reliable and accurate single-molecule force measurements. Using DNA self-assembly techniques, we have nanoengineered a unique linker that behaves as a force-activated single-molecule switch. This switch changes conformation under force to signify bond rupture, providing an identifiable molecular signature that eliminates the possibility of accidentally measuring non-specific, multiple and unknown interactions. Furthermore, this construct enables the same pair of interacting molecules to be brought back together following rupture, opening the way to high-throughput serial measurements, single-molecule on-rate studies, and studies of population heterogeneity. Our approach is simple, versatile and modular, and can be easily implemented using standard commercial reagents and laboratory equipment. We elaborate on this approach in section 1.1, and provide an overview of standard linker geometries for single-molecule manipulation experiments.

1.1. Overview of linker geometries in single-molecule experiments

A variety of different linker strategies have been employed in single-molecule experiments. These include different chemical attachment strategies (e.g. SMCC, click chemistry, EDC, etc), surface preparations (e.g. silanization methods), and linkage

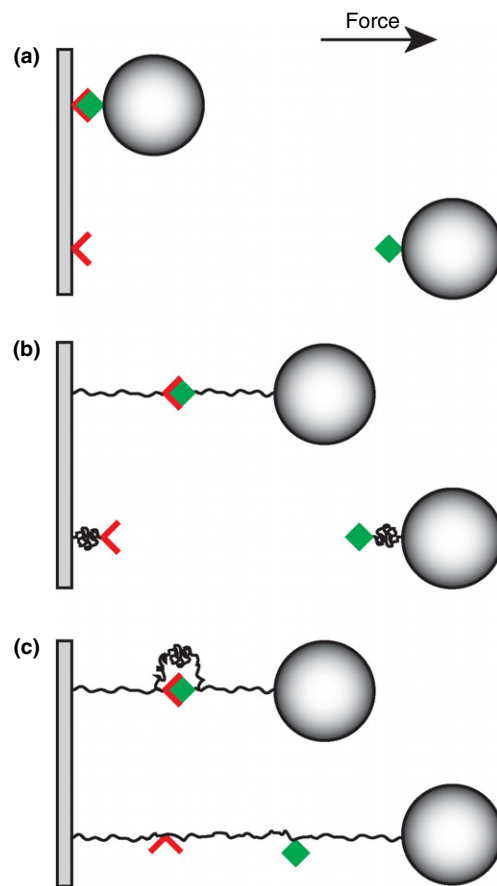


Figure 2. Single-molecule linking geometries: a cartoon showing receptor–ligand unbinding using a variety of linking strategies including (a) direct contact/a short linker, (b) a long linker, and (c) a looped linker.

materials (e.g. DNA, PEG) [14–18]. Most of these approaches can be classified into a few basic categories based on their geometry (figure 2). In this subsection, we review these categories, and show how appropriately designed linkages can improve the efficiency and reliability of single-molecule rupture measurements.

(a) *Direct contact/short linkers.* First, we consider the simplest strategy of direct molecular coating onto a surface (figure 2(a)), which is typically accomplished via adsorption or conjugate chemistry with short linkers (e.g. SMCC, EDAC). This approach has been commonly used, particularly in early single-molecule experiments [19, 9]. Some advantages of this approach are that it is typically simple, fast and inexpensive, particularly for the case of physical adsorption of molecules and cells to a surface. However, the first major problem that arises from this geometry is the introduction of unwanted interactions with the surfaces. Since the sample molecules are typically located within nanometers of the surfaces, non-specific surface–surface and molecule–surface interactions (e.g. van der Waals and depletion forces) may significantly affect the measured force [20]. Furthermore, any impurities or contamination in the sample may result in unwanted and unidentifiable adhesion between the surfaces. To deal with these difficulties, careful characterization and minimization of

non-specific interactions are necessary. Reduction of non-specific adhesion can be accomplished by blocking agents such as BSA, casein, Pluronic F127, and Tween, but they are often difficult to eliminate completely. For bond rupture measurements, the second difficulty with this geometry is the lack of a specific mechanical signature for the molecule of interest. Thus, detachment events arising from both multiple attachments and non-specific attachments are difficult to distinguish from the single-molecule interaction of interest. Minimization of multiple attachments can be accomplished by diluting the active molecules on the surfaces, and by controlling the distance, touch time and touch force between the functionalized surfaces during the experiment. While careful control experiments and the use of statistical techniques to estimate the number of single bonds can help to mitigate difficulties arising from direct contact geometry [21], we will see that the use of longer linkers can improve the reliability, accuracy, and ease of analysis of the resulting single-molecule data.

(b) *Long linkers.* A variety of linking strategies have been developed for keeping the molecules of interest far from the surfaces to which they are attached (figure 2(b)). This can be accomplished using long polymer linkers such as PEG [17] or DNA [16], or with more exotic materials such as the M13 filamentous bacteriophage [22]. Long linkers can serve the double purpose of both eliminating close range non-specific interactions and facilitating the positive identification of each tether as a single molecule; the required linker length depends upon the resolution of the force-probe instrument and the compliance of the molecule of interest. When used on one side, a sufficiently long linker can already eliminate surface-surface non-specific interaction, as well as allowing positive identification of a single interaction by using the known force-extension behavior of the tether. When used on both sides as depicted in figure 2(b), the linkers can additionally eliminate non-specific surface-molecule interactions. We note that long linkers between the force probe and the molecule of interest may complicate the force-loading history and effective energy landscape, but this can generally be accounted for [23, 15].

(c) *Looped linkers.* More recently, single-molecule experiments have been performed using a looped linker geometry, in which the interacting molecules/sites of interest are connected to each other by a molecular tether [24, 25]. This looped linker geometry as shown in figure 2(c) has two primary advantages. First, it provides an additional signature for bond rupture events, as this molecular transition will create a well-defined increase in the tether length. Unlike for the non-looped geometries, unbinding of the receptor-ligand pair cannot be confused with accidental unbinding from the anchoring ends. Second, the looped linker allows for repeated testing of the exact same pair of molecules, provided the conditions for reforming the bond are favorable. This opens up new possibilities for studying population heterogeneity in a population of molecules—a highly useful, but difficult to realize, benefit of single-molecule experiments. This looped linker concept was recently introduced as ReaLiSM (receptor and ligand in a single molecule) [24], where the A1 domain of the von Willebrand factor was linked by an amino acid chain

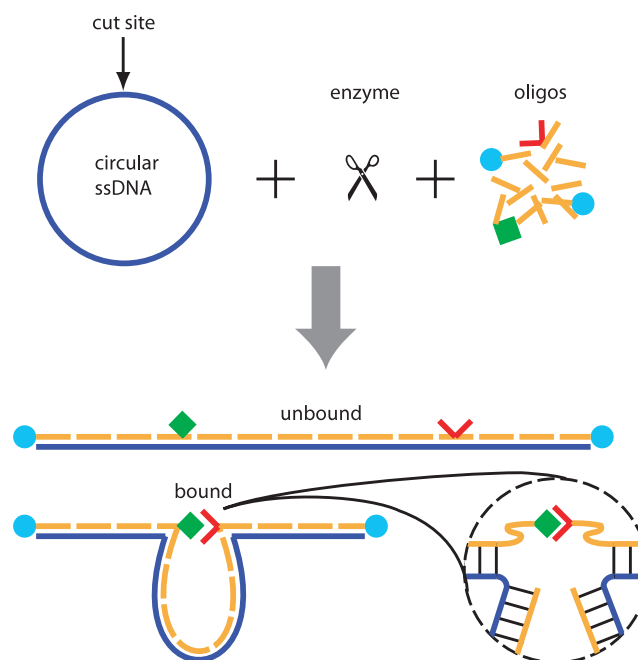


Figure 3. Looped linker construction using DNA origami: circular single-stranded DNA is enzymatically cleaved at a single site and mixed with over 100 oligonucleotides to self-assemble into a looped linker with functional groups. Supplemental figure 2 (available at stacks.iop.org/Nano/22/494005/mmedia) shows a similar construct looped with a single 'bridge' oligo.

to platelet GPIIb/IIIa, and the two interacting protein domains were repeatedly bound and unbound. While highly effective, the ReaLiSM construct as presented may be difficult for many labs to create, requiring expertise in protein engineering and purification.

Here we present a versatile DNA-based alternative constructed using DNA origami methods [26, 27]. By mixing a long piece of single-stranded DNA with a carefully designed soup of short DNA oligomers, we have constructed looped single-molecule linkers with an integrated receptor-ligand pair via DNA self-assembly (figure 3).

2. Materials and methods

2.1. Linker design and construction

Two different kinds of linkers were designed and assembled based on techniques outlined from previous DNA origami work [26, 27]. Both linkers incorporate functional 'sticky' ends (we used double biotin on both ends) which act as anchors for single-molecule experiments, as well as two functional sites near the middle of the linker to form the loop. One set of constructs forms the loop by hybridizing a single 'bridge' oligo across two distinct locations, while the other set used two separate oligos each functionalized with digoxigenin or anti-digoxigenin, which can bind to each other as a receptor-ligand pair to form the loop.

To make these linkers, M13mp18 single-stranded DNA (New England Biolabs) was first linearized by hybridizing a 40-nucleotide oligo to form a double-stranded region and then cleaving this region with BtsCI restriction enzyme (New

England Biolabs). The linearized single-stranded DNA was then mixed with complimentary oligos (Bioneer, Inc.) and subjected to a temperature ramp from 90 to 20 °C with a 1 °C min⁻¹ ramp in a PCR machine (Bio-Rad) to allow the oligos to anneal properly. For the linker with the bridge oligo formed loop, 121 oligos excluding the bridge oligo were added in tenfold molar excess, with the bridge oligo added in equimolar concentration to the scaffold strand. For the receptor–ligand loop construct, 120 oligos excluding the antibody oligo were in tenfold molar excess, which was added in equimolar concentration and subjected to a temperature ramp from 40 to 10 °C with a 0.5 °C min⁻¹ ramp after the other 120 were linked.

Detailed protocols and the full sequences of all oligos are available in the supplemental information (available at stacks.iop.org/Nano/22/494005/mmedia). All oligos were purchased from Bioneer, Inc., with the exception of the 5' double-biotin oligo (Integrated DNA Technologies), the digoxigenin oligos (Integrated DNA Technologies), and a few plain oligos ordered with next-day service (Invitrogen).

2.2. DNA–protein conjugation

A 3' thiol modified oligo was reduced and linked to monoclonal and polyclonal anti-digoxigenin (Roche Applied Science) using sulfo-SMCC (Pierce) and the accompanying protocol. The NHS group on the SMCC was first linked to free amines on the antibody (at 1 mg ml⁻¹) with a 30 min reaction at room temperature using 20-fold molar excess of SMCC in PBS at pH 7.4. At the same time, the thiol oligo was deprotected and reduced by incubating in 50 mM TCEP (Pierce) for 20 min and then cleaned using a PCR clean up kit (Qiagen). Following the first SMCC reaction, excess SMCC was removed with a Zeba desalting column (Pierce), pre-equilibrated with PBS buffer. The activated protein was then mixed with the reduced thiol oligo in a 1:1 molar ratio for 30 min at RT.

Conjugation was verified by visualization on a 4–20% polyacrylamide gel (Bio-Rad) run in 1 × TBE buffer at 150 V for 40 min, where a shift from the protein linkage was readily apparent (see supplemental figure 3 available at stacks.iop.org/Nano/22/494005/mmedia). Typically, 5–50% of the oligos were conjugated to protein, and purification of the protein–DNA conjugate was accomplished by excising the gel band and using an electro-elution kit with the accompanying protocol (Gerard biotech).

2.3. Single-molecule force spectroscopy

The final unpurified linkers with double-biotin ends were incubated with streptavidin polystyrene beads (Corpuscular) for 15 min, and then injected into a chamber with PBS buffer for use in the optical trap. The optical trap setup consists of a single stationary trap and a piezo-controlled micropipette integrated into an inverted light microscope (Nikon). The setup is functionally identical to previously described instruments [6, 28], but with 160× overall magnification instead of 400×. High-speed video microscopy is used to measure bead positions in 1D with a resolution of ~4 nm at ~2 kHz. The optical trap is calibrated using

the blur-corrected power spectrum fit [29], with additional calibration information provided by the dsDNA overstretching transition [30].

Single-molecule force measurements are performed by bringing linker functionalized beads held in the optical trap into contact with streptavidin-coated beads held in the micropipette to form molecular tethers. Tension in each tether is applied by moving the bead in the micropipette, and quantified by measuring the displacement of the bead in the optical trap. The observed distance between the beads gives a measure of the tether length.

3. Results and discussion

We successfully created looped single-molecule linkers via DNA self-assembly. Two different kinds of linker constructs were generated and tested: (i) linkers looped by a short complementary strand of DNA to study the kinetics of DNA base pairing, and (ii) linkers looped by a receptor–ligand pair to study protein–protein interactions. As detailed below, the proper assembly and functionality of these linkers was verified using gel-shift assays and optical trap measurements. We demonstrated their effectiveness for single-molecule force spectroscopy by measuring the kinetics of bond rupture for both DNA hybridization and an antibody–antigen interactions, and by showing how the molecular signature of a looped tether can be used to improve the accuracy of the data.

3.1. Verification of the linker assembly

We first tested the linkers looped by a single DNA oligo bridge, as they served as a good model system for testing and optimizing linker assembly, independent of protein-coupling efficiency. For these oligo bridge constructs, we made two different loop lengths: 2580 base pairs and 600 base pairs. Additionally, we varied the length of the bridge oligo on one side to be 30 bp, 20 bp, 15 bp, and 10 bp, while the other side was maintained at 30 bp. The formations of both long and short loops were easily distinguishable from those of unlooped products by a gel shift due to slower migration on a 0.7% agarose gel (figure 4), for both the 30 bp and 20 bp bridge constructs. We were unable to observe any looped construct in the gel when using the 15 bp or 10 bp bridge oligo, presumably due to the harsh conditions of electrophoresis (e.g. low salt, high temperature, high voltage). Confirmation that the shifted gel band was indeed the looped construct was accomplished by cutting the construct with a single-cut enzyme in the loop region (figure 4)—the shifted band (looped DNA) was largely unaffected by the enzyme, while the lower band (unlooped DNA) was completely digested into two separate pieces.

Next, these products (with double-biotin ends) were verified directly in the optical trap by pulling them end to end with linear ramps of force (figure 4). Unlooped linkers show characteristic DNA force–extension behavior with typical contour lengths of 2000–2300 nm, consistent with the number of DNA bases within the construct. The looped linkers initially start with a shorter contour length, then exhibit a sudden increase to this full contour length when the DNA

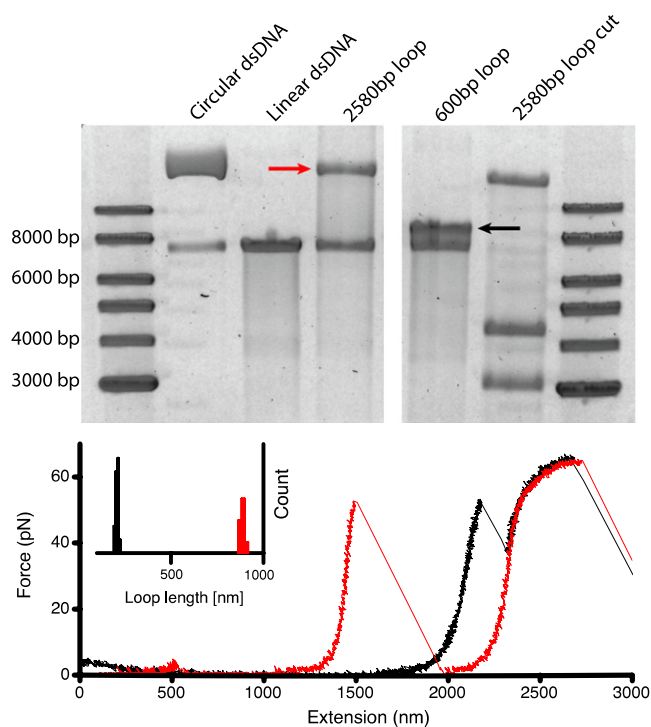


Figure 4. Verification of DNA bridge looped linker. Top: gel electrophoresis on a 0.7% agarose gel at 5 V cm^{-1} for 2 h, stained with Sybr gold. Bottom: single-molecule pulling trajectories demonstrating the sudden increase in tether length that signifies bond rupture events. The inset shows a histogram of the change in tether length for the 2580 bp (red) and 600 bp (black) looped linkers.

bridge ruptures under the application of mechanical stress. We measured an average increase in contour length of 884 nm and 208 nm for the long and short loops, respectively (figure 4 inset), which is within a few nanometers of the expected length changes of 877 and 204 nm predicted from the worm-like chain polymer model using a contour length of 0.34 nm per base pair [31, 3]. As can be seen in figure 4, after bridge rupture both curves roughly follow the curve for the unlooped linker. As the linker was stressed above 65 pN, the DNA overstretching transition could be observed, which served as an additional mechanical signature for identifying single-molecule tethers. However, pulling the molecule through this transition always resulted in detachment of the linker from the functionalized beads, presumably due to the force-induced melting of the biotinylated anchor oligos off of the ssDNA scaffold. While this effectively limits the use of this linker to measurements below about 65 pN, this could likely be overcome by covalently cross-linking the DNA linker or by using much longer anchoring oligos. Regarding the observed length of the linkers, we note that a distribution of lengths is expected from multiple-tether measurements, even if every tether is identical on a molecular level. Since the bead in the pipette is rotationally constrained, tethers may be held at different angles, causing the measured distance between the beads to differ from the molecular tether length.

Receptor–ligand looped linkers were also created in order to measure the force-dependent kinetics of an antibody–antigen interaction. Oligos coupled to digoxigenin and to

its antibody were assembled to form linkers with a loop length of 600 base pairs. The verification of these constructs was conducted in the same way as for the DNA bridge looped linkers, using both gel electrophoresis shift assays and single-molecule pulling experiments. We note that while the polyclonal looped constructs could be readily seen in a gel as a distinct shifted band (identical to the DNA bridge looped construct in figure 4), the monoclonal constructs could not. This is likely due to the much lower affinity between digoxigenin and its monoclonal antibody, and is consistent with the lack of a band for the 10 bp and 15 bp DNA bridge constructs. However, both the monoclonal and polyclonal constructs could be observed in the optical trap, and exhibited force–extension curves that matched those of the 600 bp oligo bridge construct.

3.2. Demonstration of single-molecule force spectroscopy

We tested the dynamic strength of DNA hybridization with the optical trap by repeatedly applying linear force ramps to the DNA bridge constructs to determine the distribution of the rupture force. The molecular signature of the looped linker serves as a powerful filtering method to distinguish the rupture of the DNA bridge from non-specific, unknown and multiple interactions. This is illustrated in figure 5 (left) for the rupture force of the 20 bp bridge, where positive identification of the correct rupture transition (using the change in tether length, overall tether length, and overstretching of the linker) enabled the removal of erroneous data that accounted for 57% (34/60) of the measured events. In the resulting data, we measured a mean rupture force of 52 pN with a standard deviation of 6 pN at a nominal loading rate of 100 pN nm^{-1} (this was a combination of experiments with a mean loading rate of 98 pN nm^{-1} and a standard deviation of 35 pN nm^{-1}). This agrees within error with the expected force of $39 \pm 15 \text{ pN}$ for the mechanical shearing of DNA (based upon their empirical formula) [12].

When testing the other DNA bridge lengths, we observed fewer rupture events for the 30 bp bridge, as the biotin–streptavidin bonds anchoring the linker would often rupture first. In addition, we also saw evidence of the 15 bp and 10 bp bridges in single-molecule pulling experiments, despite not seeing these constructs with the gel-shift assay. While the formation of these loops should be energetically favorable even with the additional entropic cost of closing the loop [32], it is possible that the conditions of electrophoresis lower the stability of these constructs leading to their absence in the gel assays.

As another demonstration, we measured the force-dependent unbinding kinetics of digoxigenin with its antibody in the optical trap (figure 5 (right)). By making repeated measurements of bond rupture under a constant force, we found a characteristic lifetime of 1.3 s (with a 95% confidence band of 0.9–2.0 s) at a force of $49 \pm 2 \text{ pN}$ for the polyclonal antibody, using maximum likelihood estimation with an exponential decay model. We found this interaction to be relatively strong, in agreement with other single-molecule measurements that used it as a molecular anchor [22]. We

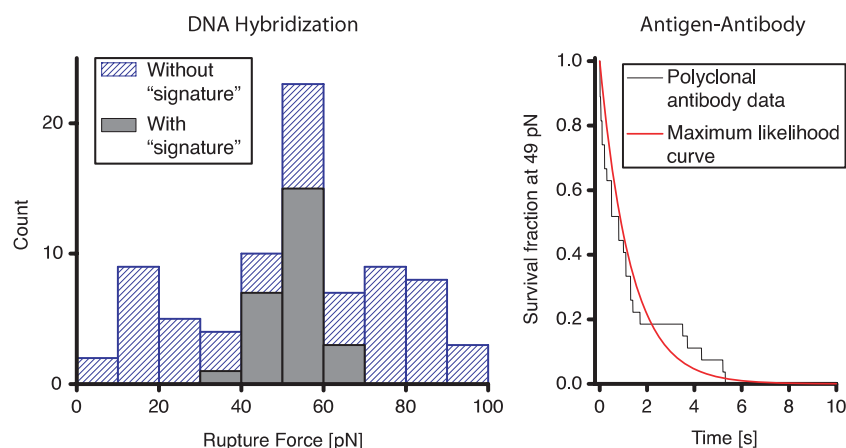


Figure 5. Single-molecule force spectroscopy results for the rupture of (left) DNA hybridization and (right) antibody–antigen interactions. Left: rupture force histogram for shearing a 20 bp DNA segment, demonstrating the filtering of erroneous data via the looped linker molecular signature. Right: survival trajectory for digoxigenin against its antibody under constant force, with results of maximum likelihood estimation superimposed.

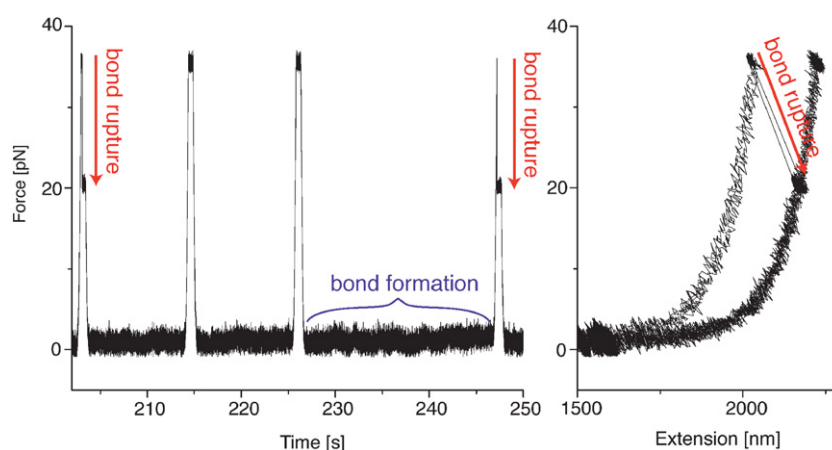


Figure 6. Trajectory demonstrating repeated rupture and formation of a single receptor–ligand pair (digoxigenin with its monoclonal antibody): (left) force versus time and (right) force versus extension traces for repeated cycles of force application and release. Bond rupture events are observable by a sudden drop in force and an increase in tether length, as demarcated by red arrows. Rebinding/bond formation during a low force clamp can be observed by subsequent bond rupture under the application of force.

note that without the looped linker the high bond strength of this interaction can make rupture measurements difficult, as it can be difficult to distinguish the rupture of digoxigenin–antibody from the failure of molecular anchors in the absence of an additional molecular signature.

Not only were we able to measure bond rupture, but single-molecule bond formation could also be observed. In many cases with the digoxigenin–antibody construct, we were able to reform the complex after dissociation by bringing the beads closer together and waiting for a short time (figure 6). However, we were not able to reform the oligo bridge after rupture under similar conditions, suggesting that the formation of secondary structure or the extra time to diffusively align the two strands slowed the rebinding kinetics.

4. Conclusion

We have presented a simple and effective method for making functional looped linkers using DNA self-assembly, which can

increase the accuracy and reliability of single-molecule force measurements. The method is versatile enough to be useful for a wide range of molecular interactions, and simple enough to be made by researchers of diverse backgrounds without significant investment of time or money (see the appendix). We demonstrated this functionality by constructing and testing two different looped linkers, designed for studying the dynamic strength of DNA base pairing and receptor–ligand interactions. In addition, we showed how the molecular signature provided by this ‘DNA mechanical switch’ enables the removal of erroneous data that can arise from non-specific, unknown, and multiple interactions. Not only is this construct useful for traditional bond rupture measurements and force spectroscopy, but it also enables the same pair of interacting molecules to be brought back together following rupture, opening the way toward high-throughput serial measurements, single-molecule on-rate studies, and studies of population heterogeneity.

Acknowledgments

The authors would like to thank Teresa Kao and Daniel Cheng for laboratory support, and William Shih and Ted Feldman for helpful discussions. This work was supported by the Rowland Junior Fellows program.

Appendix. Practical considerations for the construction of looped linkers

The goal of this work was to develop a looped single-molecule linker, with an easily identifiable molecular ‘signature’, that is both versatile and easy to implement. While the DNA origami construction of the linker may sound intimidating due to the sheer quantity of oligos used, it is rather simple in practice. We recommend dividing the ssDNA scaffold into fixed and variable regions. The variable regions are those that may be changed in the future to have different labels, while the fixed regions will only have unlabeled oligos. Then all of the ‘fixed’ oligos can be ordered pre-mixed to save time and eliminate the possibility of mixing error (Bioneer was accommodating in this regard). In our case, we designated 12 variable oligos each spaced apart by 9–10 fixed oligos, and ordered the 109 fixed oligos pre-mixed in a single tube. The variable oligos gave us the flexibility to choose different oligo labels and to choose different loop lengths for our construct, without significant protocol modification.

The choice of oligo length should also be considered. We chose 60 nucleotide oligos to minimize the number of oligos needed (companies vary in maximum oligo size), but in hindsight the pre-mixing of the fixed oligos makes the number of oligos less important. The main differences to consider with shorter oligos will be differences in annealing behavior, requisite protocol modifications, and price. Regarding annealing, longer oligos have higher melting temperatures, which should increase the annealing speed in a decreasing temperature ramp. On the other hand, longer oligos tend to have more secondary structure which can sometimes impede proper annealing, especially at lower temperatures. Regarding protocol modification, oligos that are 30 bp or shorter can be washed out with PCR clean up kits, which would necessitate the use of a different cleaning method in our SMCC conjugation. Regarding price, the yield of shorter oligos can be significantly higher, making them more cost effective.

It is worth considering cost in more detail, as it could be a deciding factor in the use of these linkers. The cost of oligos continues to decrease, and many companies offer discounts for large oligo orders or those ordered in plates instead of individual tubes. As an example, our construct cost under \$1000 with unmodified oligos. Modified oligos will increase the cost depending on the modification, from tens to hundreds of dollars per oligo. However, this initial investment can produce several liters of product at the nanomolar concentrations that are typically required for single-molecule experiments. Surprisingly, the most expensive ingredient on a molar basis when using short unpurified and unmodified oligos is the M13 scaffold [26].

To generate linkers of different lengths, alternative ssDNA scaffolds could be used. For example, ssDNA can be generated using asymmetric PCR, or obtained by strand-separating standard PCR products. Product from rolling-circle amplification could also be used for the generation of periodic linkers. An alternative method for constructing looped linkers that we have been exploring is ligating together the products of multiple PCR reactions.

Lastly, we will discuss the time, equipment, and expertise requirements for making these linkers, as these were primary considerations for us in starting this project. By following the protocols in the methods section (described in detail in the supplemental information available at stacks.iop.org/Nano/22/494005/mmedia), the linkers can be completely constructed and verified in a single working day, and this time could probably be reduced with further optimization. The protein conjugation procedure takes about 2–3 h, with an additional 2 h for purification. The oligo annealing process (excluding protein-conjugated oligos) takes 70 min, and can be done in parallel with the protein conjugation step. Annealing the protein-conjugated oligo(s) takes another 1 h, and final verification of the looped linker on a gel takes an additional 1–2 h. Overall, it can be done in 6–8 h from start to finish. The equipment requirements are minimal, and the protocols can be carried out with only modest pipetting skills. The only major equipment needs are for a centrifuge, and horizontal and vertical electrophoresis systems (the vertical one was used for protein–oligo purification, but we have seen gel shifts in agarose as well). We used a PCR machine for the annealing protocol, but this is not strictly necessary and could be replaced with a hot water bath cooling slowly to room temperature. All reactants and kits used are commercially available.

These linkers are intended to be versatile for studying a variety of molecules, and in fact much of the protocols will remain the same even as specific molecules on the linker are changed. The modularity of the linker makes it simple to use different proteins by just swapping one functionalized oligo for another. If the linker is constructed with only the protein-conjugated oligos omitted, this stock solution of partially constructed linker can then be mixed with the specific protein oligos to get the final construct. The only additional step required will be to repeat the chemical conjugation of oligo to protein for each specific case. In our example linkers, we used SMCC, but there are a variety of other bioconjugation techniques that could be used instead. In the case of antibodies, it is also possible to use antibody binding proteins such as protein G to simplify the process of swapping in different antibodies.

References

- [1] Deniz A A, Mukhopadhyay S and Lemke E A 2008 Single-molecule biophysics: at the interface of biology, physics and chemistry *J. R. Soc. Interface* **5** 15
- [2] Ritort F 2006 Single-molecule experiments in biological physics: methods and applications *J. Phys.: Condens. Matter* **18** R531
- [3] Bustamante C, Bryant Z and Smith S B 2003 Ten years of tension: single-molecule DNA mechanics *Nature* **421** 423–7

- [4] Svoboda K, Schmidt C F, Schnapp B J and Block S M 1993 Direct observation of kinesin stepping by optical trapping interferometry *Nature* **365** 721–7
- [5] Greenleaf W J, Woodside M T and Block S M 2007 High-resolution, single-molecule measurements of biomolecular motion *Annu. Rev. Biophys. Biomol. Struct.* **36** 171
- [6] Zhang X, Halvorsen K, Zhang C Z, Wong W P and Springer T A 2009 Mechanoenzymatic cleavage of the ultralarge vascular protein von Willebrand factor *Science* **324** 1330
- [7] Evans E 2001 Probing the relation between force–lifetime–and chemistry in single molecular bonds *Annu. Rev. Biophys. Biomol. Struct.* **30** 105–28
- [8] Kufer S K, Puchner E M, Gump H, Liedl T and Gaub H E 2008 Single-molecule cut-and-paste surface assembly *Science* **319** 594
- [9] Neuman K C and Nagy A 2008 Single-molecule force spectroscopy: optical tweezers, magnetic tweezers and atomic force microscopy *Nature Methods* **5** 491–505
- [10] Halvorsen K and Wong W P 2010 Massively parallel single-molecule manipulation using centrifugal force *Biophys. J.* **98** L53–5
- [11] Evans E and Ritchie K 1997 Dynamic strength of molecular adhesion bonds *Biophys. J.* **72** 1541–55
- [12] Strunz T, Oroszlan K, Schäfer R and Güntherodt H J 1999 Dynamic force spectroscopy of single DNA molecules *Proc. Natl Acad. Sci.* **96** 11277
- [13] Evans E A and Calderwood D A 2007 Forces and bond dynamics in cell adhesion *Science* **316** 1148
- [14] Hermanson G T 2008 *Bioconjugate Techniques* 2nd edn (New York: Academic)
- [15] Friedsam C, Wehle A K, Kühner F and Gaub H E 2003 Dynamic single-molecule force spectroscopy: bond rupture analysis with variable spacer length *J. Phys.: Condens. Matter* **15** S1709
- [16] Hegner M 2000 DNA handles for single molecule experiments *Single Molecules* **1** 139–44
- [17] Hinterdorfer P, Gruber H J, Kienberger F, Kada G, Riener C, Borken C and Schindler H 2002 Surface attachment of ligands and receptors for molecular recognition force microscopy *Colloids Surf. B* **23** 115–23
- [18] Perret E, Leung A, Morel A, Feracci H and Nassoy P 2002 Versatile decoration of glass surfaces to probe individual protein–protein interactions and cellular adhesion *Langmuir* **18** 846–54
- [19] Lee G U, Kidwell D A and Colton R J 1994 Sensing discrete streptavidin–biotin interactions with atomic force microscopy *Langmuir* **10** 354–7
- [20] Israelachvili J N 1992 *Intermolecular and Surface Forces: With Applications to Colloidal and Biological Systems* (New York: Academic)
- [21] Evans E, Halvorsen K, Kinoshita K and Wong W P 2009 A new approach to analysis of single-molecule force measurements *Handbook of Single-Molecule Biophysics* (Dordrecht: Springer) pp 571–89
- [22] Khalil A S, Ferrer J M, Brau R R, Kottmann S T, Noren C J, Lang M J and Belcher A M 2007 Single M13 bacteriophage tethering and stretching *Proc. Natl Acad. Sci.* **104** 4892
- [23] Evans E and Ritchie K 1999 Strength of a weak bond connecting flexible polymer chains *Biophys. J.* **76** 2439–47
- [24] Kim J, Zhang C Z, Zhang X and Springer T A 2010 A mechanically stabilized receptor–ligand flex-bond important in the vasculature *Nature* **466** 992–5
- [25] Wiita A P, Ainavarapu S R K, Huang H H and Fernandez J M 2006 Force-dependent chemical kinetics of disulfide bond reduction observed with single-molecule techniques *Proc. Natl Acad. Sci.* **103** 7222–7
- [26] Rothmund P W K 2006 Folding DNA to create nanoscale shapes and patterns *Nature* **440** 297–302
- [27] Douglas S M, Dietz H, Liedl T, Högberg B, Graf F and Shih W M 2009 Self-assembly of DNA into nanoscale three-dimensional shapes *Nature* **459** 414–8
- [28] Halvorsen K 2007 Probing weak single-molecule interactions: development and demonstration of a new instrument *PhD Thesis* Boston University, Massachusetts
- [29] Wong W P and Halvorsen K 2006 The effect of integration time on fluctuation measurements: calibrating an optical trap in the presence of motion blur *Opt. Express* **14** 12517–31
- [30] Smith S B, Cui Y and Bustamante C 1996 Overstretching b-DNA: the elastic response of individual double-stranded and single-stranded DNA molecules *Science* **271** 795
- [31] Bustamante C, Marko J F, Siggia E D and Smith S 1994 Entropic elasticity of lambda-phage DNA *Science* **265** 1599–600
- [32] Hanke A and Metzler R 2003 Entropy loss in long-distance DNA looping *Biophys. J.* **85** 167–73